

Lateral phase separation of confined membranes

Mesfin Asfaw

Molecule and Life Nonlinear Sciences Laboratory, Research
Institute for Electronic Science, Hokkaido University, Kita 20 Nishi 10, Kita-ku,
Sapporo 001-0020, Japan

November 12, 2018

Received: date / Revised version: date

Abstract

We consider membranes interacting via short, intermediate and long stickers. The effects of the intermediate stickers on the lateral phase separation of the membranes are studied via mean-field approximation. The critical potential depth of the stickers increases in the presence of the intermediate sticker. The lateral phase separation of the membrane thus suppressed by the intermediate stickers. Considering membranes interacting with short and long stickers, the effect of confinement on the phase behavior of the membranes is also investigated analytically.

1 Introduction

Membranes serve a number of general functions in our cells and tissues. They separate cells and cell compartments [1, 2]. They act as barriers as their lipid core is permeable to water and to small hydrocarbon molecules and relatively impermeable to macromolecules and polar molecules. In addition, membrane proteins facilitate or assist the transport of ions and macromolecules into and out of the cells. Since biomembranes play a vital role in biological process, they have

attracted significant experimental and theoretical interest [3, 4, 5, 6]. The physics of membrane adhesion is one of the aspects that has got considerable attention [7, 8, 9, 10, 11, 12, 13, 14, 15, 16, 17]. Recent experimental realization [18] uncovers the formation of domains between short and long receptors of T cells. The dynamics of adhesion induced phase separation was also considered theoretically in the works [19, 20] and its detailed equilibrium studies were reported in the previous studies [22, 23, 24]. All these theoretical and experimental investigations have significantly contributed to the basic understanding of the physics of membranes. More recently, we presented a theoretical study for adhesion-induced lateral phase separation of membranes with short stickers, long stickers and repellers confined between two hard walls [25]. The effects of confinement and repellers on lateral phase separation were investigated. It is found that the sticker critical potential depth tends to increase as the distance between the hard walls decreases which suggests confinement-induced or force-induced mixing of stickers.

Despite the success to understand the thermodynamic properties of these non-homogeneous membranes, more efforts are needed to get a complete picture of the physics of membranes due to the fact that membranes contain large number of macromolecules which are organized in complex fashion. Most of the recent works considered membranes interacting with one or two types of stickers (receptor/ligand pairs). However the adhesive molecules may have different resting length; the experimental investigations of T cells unveiled two or more receptor-ligand pairs being involved in the binding process [15]. Another crucial issue on the adhesion induced lateral phase separation is the effect of confinement. Cell adhesion often occurs in the presence of external force field due to external flow [25]. The aim of this work is to investigate the phase behavior of confined membranes interacting with more than one types of stickers. First we investigate the phase behavior of membranes with short and long stickers analytically which can be taken as an independent check of the results found in the previous works [24, 25]. We then extend our previous studies by considering membranes interacting with three adhesive molecules.

The rest of the work is structured as follows. In section II, we introduce our model. In section III, we present the mean field approximation while section IV and V deal with membranes interacting via two and three types of stickers, respectively. Section VI deals with summary and conclusion.

2 The model

We consider non-homogenous membrane that interacts via receptor/ligands (stickers) of different characteristic length as shown in Fig. 1. For simplicity, a discretized membrane (lattice gas model [12, 24]) with lattice constant a is considered. The separation field l separates the membrane from the membrane (substrate) while the occupation number $n_i = 0$ shows no sticker present at the lattice site i while $n_i = 1, 2, 3\dots$ indicates the presence of stickers 1, stickers 2, stickers 3... at lattice site i , respectively (see Fig. 1).

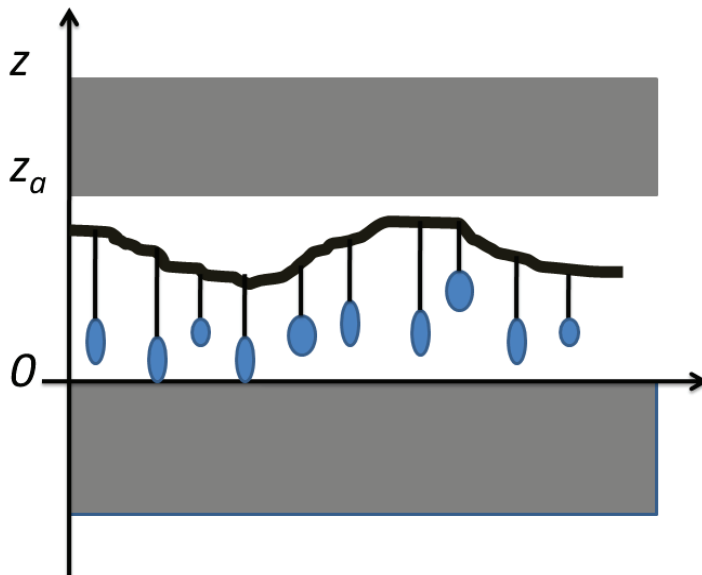


Figure 1: Schematics diagram of membrane with stickers of different size near to a substrate. z denotes the local separation field that separates the membrane from the substrate.

Introducing the rescaled fields $z = (l/a)\sqrt{k/T}$ and $V = V/T$ reduces the number of independent parameters. For tensionless non-homogenous multi-component membranes, the Hamiltonian of the model is given by

$$H[z, n] = H_{el}[z] + \sum_i \delta_{1, n_i} (V_1(z_i) - \mu_1) +$$

$$\begin{aligned}
& \sum_i \delta_{2,n_i}(V_2(z_i) - \mu_2) + \sum_i \delta_{3,n_i}(V_3(z_i) - \mu_3) \\
& + \sum_i \delta_{4,n_i}(V_4(z_i) - \mu_4) + \dots
\end{aligned} \tag{1}$$

with the elastic term

$$H_{el}[z] = \sum_i \frac{\kappa}{2a^2} (\Delta_d z_i)^2 \tag{2}$$

where $H_{el}[z]$ denotes the discretized bending energy of the membranes with an effective bending rigidity κ . Typically, $\kappa = 10 - 20k_B T$. The discretized Laplacian Δ_d is given by $\Delta_d z_i = z_{i1} + z_{i2} + z_{i3} + z_{i4} - 4z_i$. $V_1(z_i)$, $V_2(z_i)$ and $V_3(z_i)$ denote the potentials for stickers 1, stickers 2, and stickers 3, respectively while μ_1 , μ_2 and μ_3 denote the chemical potentials for the stickers 1, stickers 2 and stickers 3, respectively. The partition function Z can be written as

$$Z = \left[\prod_i \int_{-\infty}^{\infty} dz_i \right] \left[\prod_i \sum_{n_i=0,1,2} \exp[-H[z, n]] \right]. \tag{3}$$

Tracing out the sticker degrees of freedom one gets

$$\begin{aligned}
Z &= \prod_i \int_{-\infty}^{\infty} dz_i [\exp[-H_{el}(z)] \\
& (1 + \exp[-V_1(z_i) + \mu_1] + \exp[-V_2(z_i) + \mu_2] + \\
& \exp[-V_3(z_i) + \mu_3] + \dots)].
\end{aligned} \tag{4}$$

Rearranging terms, Equation (4) can be written as

$$\begin{aligned}
Z &= (1 + \exp[\mu_1] + \exp[\mu_2] + \exp[\mu_3] + \dots)^N \\
& \prod_i \int_{-\infty}^{\infty} dz_i \exp \left[-H_{el}(z) + \sum_i [V^{eff}(z_i)] \right].
\end{aligned} \tag{5}$$

The effective potential $V^{eff}(z)$ is given by

$$\begin{aligned}
V^{eff}(z) &= -\ln[(1 + \exp[-V_1(z) + \mu_1] + \exp[-V_2(z) + \mu_2] + \\
& \exp[-V_3(z) + \mu_3] + \dots)/\xi_0]
\end{aligned} \tag{6}$$

where $\xi_0 = 1 + \exp[\mu_1] + \exp[\mu_2] + \exp[\mu_3] + \dots$. Integrating out the stickers degrees of freedom leads to a homogeneous membrane with an

effective potential which is given by Eq. (6). The stickers potential is modeled as square-well potential [12, 24]) $V_1 = U_1$ for $z_1 < z_i < z_2$, $V_2 = U_2$ for $z_3 < z_i < z_4$, $V_3 = U_3$ for $z_5 < z_i < z_6$ and $V_1, V_2, V_3 \dots = 0$ otherwise. The effective potential (6) then can be rewritten as $V^{eff} = \infty$ for $z < 0$, $V^{eff} = U_1^{eff}$ for $z_1 < z_i < z_2$, $V^{eff} = U_2^{eff}$ for $z_3 < z_i < z_4$, $V^{eff} = U_3^{eff}$ for $z_5 < z_i < z_6 \dots$ where

$$U_1^{eff} = -\ln[(1 + \exp[-U_1 + \mu_1] + \exp[\mu_2] + \exp[\mu_3] + \dots)/\xi_0], \quad (7)$$

$$U_2^{eff} = -\ln[(1 + \exp[-U_2 + \mu_2] + \exp[\mu_1] + \exp[\mu_3] + \dots)/\xi_0] \quad (8)$$

and

$$U_3^{eff} = -\ln[(1 + \exp[-U_3 + \mu_3] + \exp[\mu_1] + \exp[\mu_2] + \dots)/\xi_0]. \quad (9)$$

One should note that $z_3 > z_2$, $z_5 > z_4$ and so on, i.e. the binding wells do not overlap.

In the next section, we study the phase behavior of membranes with short and long stickers utilizing the mean field approximation.

3 Mean-field approximation

When fluctuation of the membranes not too strong, one can apply mean-field approximation to the discretized Laplacian $\Delta_d z_i = 4[z_{min} - z_i]$ where z_{min} designates the average separation field. Substituting this equation in Eq. (1), the elastic term takes a simple form: $H[z] = \sum_i (4[z_{min} - z_i])^2$. Within the mean field approximation, one can write Eq. (5) as

$$Z = (\xi_0)^N \left[\int_0^\infty dz_i \exp[-8(z_{min} - z_i)^2 - V^{eff}(i)] \right]^N. \quad (10)$$

The free energy of the membrane after some algebra is given by

$$G = -\ln \left[\int_0^\infty dz_i [\exp[-8(z_{min} - z_i)^2 - V^{eff}(i)]] / \xi_0 \right]. \quad (11)$$

Varying the free energy (11) with respect to z_{min} leads to a self-consistence equation of the form:

$$z_{min} = \frac{\int_0^\infty z \exp[-8(z_{min} - z_i)^2 - V^{eff}(i)] dz_i}{\int_0^\infty \exp[-8(z_{min} - z_i)^2 - V^{eff}(i)] dz_i}. \quad (12)$$

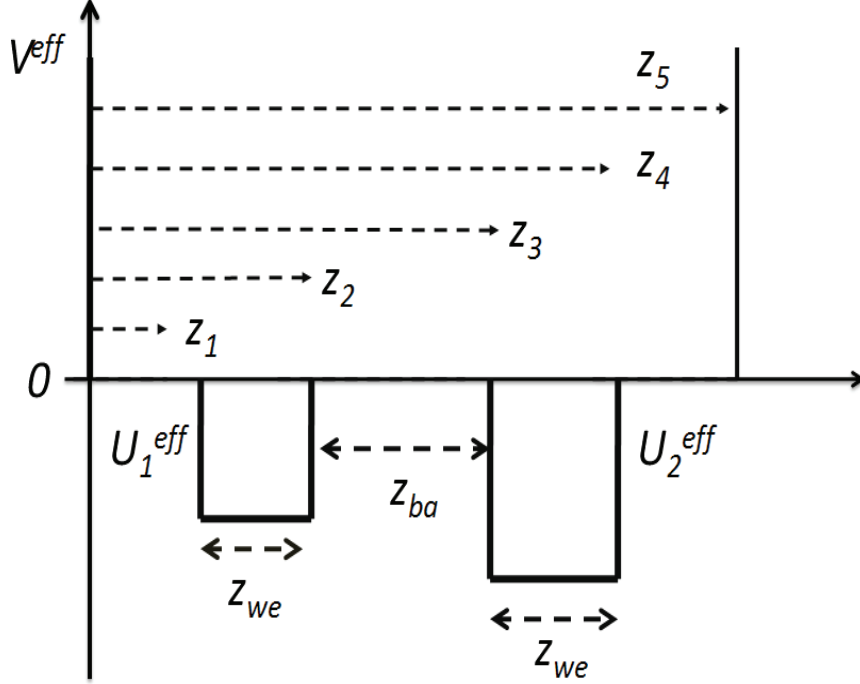


Figure 2: Double-well potential V^{eff} with two degenerate minima at both sides of the wells. The potential has two square wells of depth U_1^{eff} and U_2^{eff} within the range $z_{we} = z_2 - z_1$ and $z_{we} = z_4 - z_3$, respectively. The effective potential $V^{eff} = \infty$ for $z \leq 0$ and $z \geq z_5$. We fix $z_a = z_5 - z_4 = z_1$.

3.1 Membranes with short and long stickers

Let us now consider membranes interacting via two types of stickers whose equilibrium phase behavior are governed by an effective double-well potential with the effective depth U_1^{eff} and U_2^{eff} as shown in Fig. 2. U_1^{eff} and U_2^{eff} depend on the stickers binding energies U_1 and U_2 , respectively. Hereafter, all energetic quantities are given in unit of $k_B T$ and to make the model analytically solvable (for symmetry reason) let $z_1 = 0$, $z_4 = z_5$, $z_{we} = z_2 - z_1 = z_4 - z_3$ and $z_{ba} = z_3 - z_2$.

When membranes are confined in one of the wells of the effective double-well potential, they remain stable with respect to thermal fluctuations provided that the potential wells are deep enough, membranes exhibit two coexisting states with two average separations z_{min}

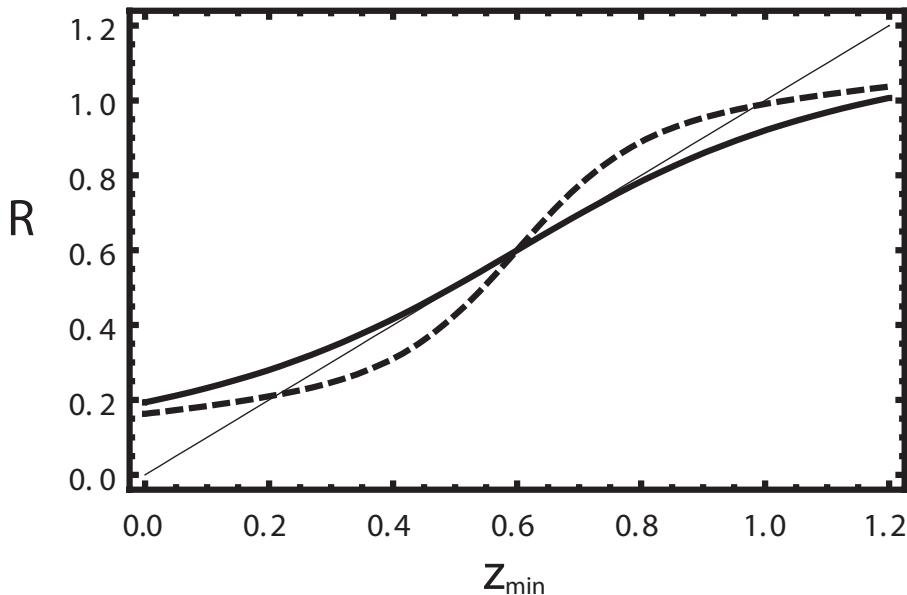


Figure 3: Graphical solution $R = \int_0^\infty z \exp[-8(z_{min} - z_i)^2 - V^{eff}(i)] dz_i / \int_0^\infty \exp[-8(z_{min} - z_i)^2 - V^{eff}(i)] dz_i$ versus z_{min} for parameter choice $z_{we} = 0.4$ and $z_{ba} = 0.4$. The dashed and the thick solid lines represent the graphical solution for $|U^{eff}| = 8$ and $|U^{eff}| = 0.2$, respectively.

[3]. In this case the membranes remain trapped in one of the wells and exhibit a first order transition. However for weak potential wells, the membrane can easily surmount the potential barrier and its average separation field $z_{min} = 0$.

At what critical potential depth U_C^{eff} do membranes confined in the double-well potential "tunnel"? This can be addressed by solving Eq. (12) numerically. For instance for parameter choice $z_{we} = 0.4$, $z_{ba} = 0.4$ and $|U^{eff}| = 8$, the graphical solution is depicted in Fig. 3. The figure clearly reveals z_{min} attending two distinct values $z_{min} = 0.2$ and $z_{min} = 0.98$ which exhibits $|U^{eff}| > |U_C^{eff}|$. On other hand for $z_{we} = 0.4$, $z_{ba} = 0.4$ and $|U^{eff}| = 0.2$, $z_{min} = 0$ revealing $|U^{eff}| < |U_C^{eff}|$ (see Fig. 3). Furthermore for parameter values of $z_{we} = 0.4$ and $z_{ba} = 0.4$, the dependence of z_{min} as a function of U^{eff} is plotted in the Fig. 4. The same figure depicts when $|U^{eff}| > |U_C^{eff}|$, membranes are confined within one of the potential wells. As the effective potential depth decreases, the tendency for membranes to stay

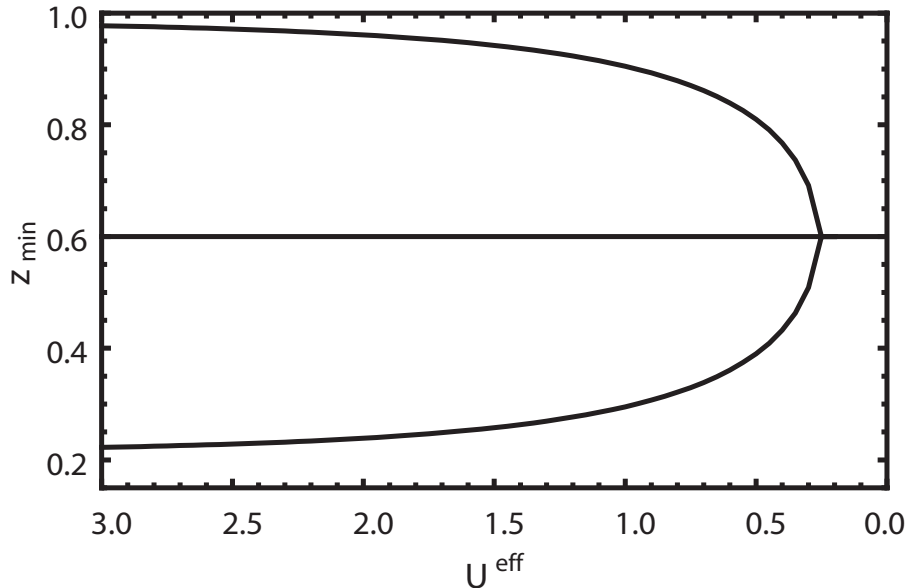


Figure 4: z_{min} versus U^{eff} for fixed $z_{we} = 0.4$ and $z_{ba} = 0.4$. The critical point is located at $|U_C^{eff}| = 0.264$. For $|U^{eff}| > 0.264$, membranes attend two different mean values while when $|U^{eff}| < 0.264$, $z_{min} = 0$.

in the potential wells decreases. When $|U^{eff}| < |U_C^{eff}|$, membranes overcome the barrier height and as the result $z_{min} = 0$.

The critical potential depth U_C^{eff} , below which phase separation occurs, can be obtained by minimizing the free energy, i.e.; $-\partial^2 G / \partial z_{min}^2 = 0$. For fixed $z_1 = 0$ and $z_4 = z_5$, one finds the critical potential depth

$$U_c^{eff} = \ln[1 - \exp[-8(z_{we}(z_{we} + z_{ba}))](1 + \frac{2z_{we}}{z_{ba}})]. \quad (13)$$

Exploiting Eq. (13), one confirms that when the potential width z_{we} steps up, U_C^{eff} declines which is consistent with the work [24, 25]. Note that z_{ba} signifies the length difference between the two stickers. As it can be readily seen in Eq. (13), when z_{ba} increases, U_C^{eff} declines. This is because when the length difference between the two stickers increases, the energy cost of keeping the short and long stickers in close proximity increases.

The effective critical potential depth U_C^{eff} relies on sticker binding energy U and stickers chemical potential μ . Comparing Eqs. (6) with

(13) and assuming $\mu_1 = \mu_2 = \mu$, one obtains the stickers critical binding energy

$$U_C = \mu - \ln\left[\frac{\beta_1}{\beta_2}\right] \quad (14)$$

where

$$\beta_1 = e^{\mu+8z_{we}(z_{we}+z_{ba})} z_{ba} + (1 + e^\mu)(z_{ba} + 2z_{we}) \quad (15)$$

and

$$\beta_2 = -1 + e^{8z_{we}(z_{we}+z_{ba})} z_{ba} - 2z_{we}. \quad (16)$$

When the stickers binding energy U_C is less than the critical binding energy $U < U_C$, the short and long stickers segregate into distinct domains while when $U > U_C$, the stickers become mixed. The dependence of U_C on model parameters can be explored via Eq. (14). When the length between short and long stickers z_{ba} as well as the width of the stickers potential z_{we} increases, the two types of stickers separate into two distinct domains at smaller critical binding energy U_C .

Let us now consider a case where $z_1 \neq 0$, $z_1 = z_5 - z_4 = z_a$ (the two wells of the effective double-well potential are far from the hard wall) as shown in Fig. 2. In this case the effective critical potential depth U_c^{eff} after some algebra is given by

$$U_C^{eff} = \ln\left[\frac{\exp[(8z_a m_1)]((\exp(8z_{we}(z_{we} + z_{ba})) - 1)z_{ba} - 2z_{we})/\alpha}{\alpha}\right] \quad (17)$$

where

$$\alpha = z_{ba} + z_{ba} \exp[(8(z_a + z_{we})m_2)] - \exp[(8z_a m_1)]z_{ba} + 2(z_a + z_{we} - \exp[(8z_a m_1)]z_{we}). \quad (18)$$

The values for m_1 and m_2 are given by $m_1 = z_{ba} + z_a + 2z_{we}$ and $m_2 = z_{ba} + z_a + z_{we}$. One can note that in the limit $z_a \rightarrow 0$, Eq. (17) converges to Eq. (13). Utilizing Eq. (17), one can see that as z_{we} and z_{ba} increase, U_c^{eff} declines which suggests that as the width of the stickers potential as well as the length between the short and long stickers increases, the stickers segregate into two distinct domains at a lower stickers critical potential depth. In the limit $z_{ba} \rightarrow \infty$ or $z_{we} \rightarrow \infty$, $|U_C| \rightarrow 0$ while in the limit $z_{ba} \rightarrow 0$ or $z_{we} \rightarrow 0$, $|U_C| \rightarrow \infty$. When z_a increases, the entropic repulsion of membranes with the wall reduces. Thus the critical potential depth of the stickers U_c^{eff} decreases which exhibits that confinement facilitates demixing of stickers and hinders lateral phase separation.

4 Membrane with short, intermediate and long stickers

Let us now consider membranes with short, intermediate and long stickers near to the substrate. Eliminating the stickers degree of freedom results in membranes interacting with triple-well potential with the effective depth U_1^{eff} , U_2^{eff} and U_3^{eff} as shown in Fig. 5. U_1^{eff} , U_2^{eff} and U_3^{eff} are function of the stickers binding energies U_1 , U_2 and U_3 , respectively. Once analyzing the effective critical potential depth, one can retrieve the critical point of the stickers binding energy.

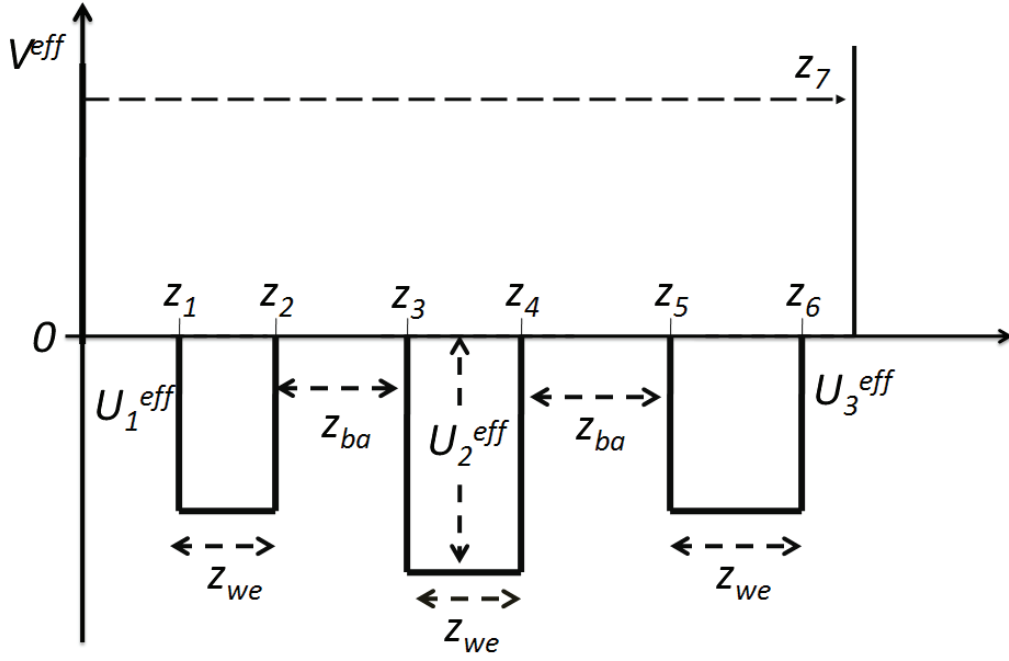


Figure 5: Triple-well potential V^{eff} with three degenerate minima. The potential has three square wells of depth U_1^{eff} , U_2^{eff} and U_3^{eff} within the range $z_{we} = z_2 - z_1 = z_4 - z_3 = z_6 - z_5$, respectively. Here $z_a = z_1 = z_7 - z_6$. The effective potential $V^{eff} = \infty$ for $z \leq 0$ and $z \geq z_7$.

Our earlier analysis unveils that for membranes with two types of stickers, the length disparity between the short and long stickers causes lateral phase separation. For pronounced length difference,

lateral phase separation occurs even at high temperature or equivalently at shallow critical potential depth. However the situation is quite different when there are intermediate stickers embedded in the membranes. The presence of intermediate stickers reduces the bending energy cost as the length gap between the short and long stickers gets diminished. Hence in the presence of additional intermediate stickers, the lateral phase separation among the stickers occurs at lower temperature or deeper critical potential depth which suggests that lateral phase separation occurs at the expense of high sticker binding energy and thus the intermediate stickers endorse mixing of stickers.

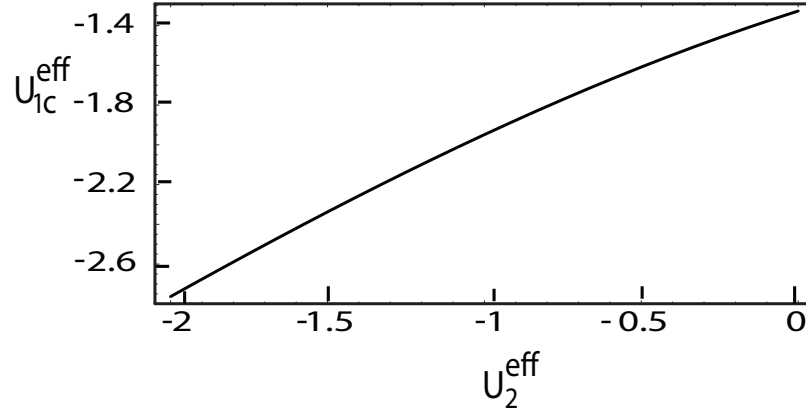


Figure 6: The critical effective potential depth $U_{1c}^{\text{eff}} = U_{3c}^{\text{eff}}$ versus U_2^{eff} for parameter choice $z_a = 0.1$, $z_{ba} = z_{we} = 0.16$.

The dependence of the critical potential depth on the model parameters can be explored numerically via Eq. (12). In order to conceive the effect of the intermediate stickers, let us vary U_2^{eff} and for simplicity let $U_1^{\text{eff}} = U_3^{\text{eff}}$. Figure 6 depicts the plot $U_{1c}^{\text{eff}} = U_{3c}^{\text{eff}}$ as

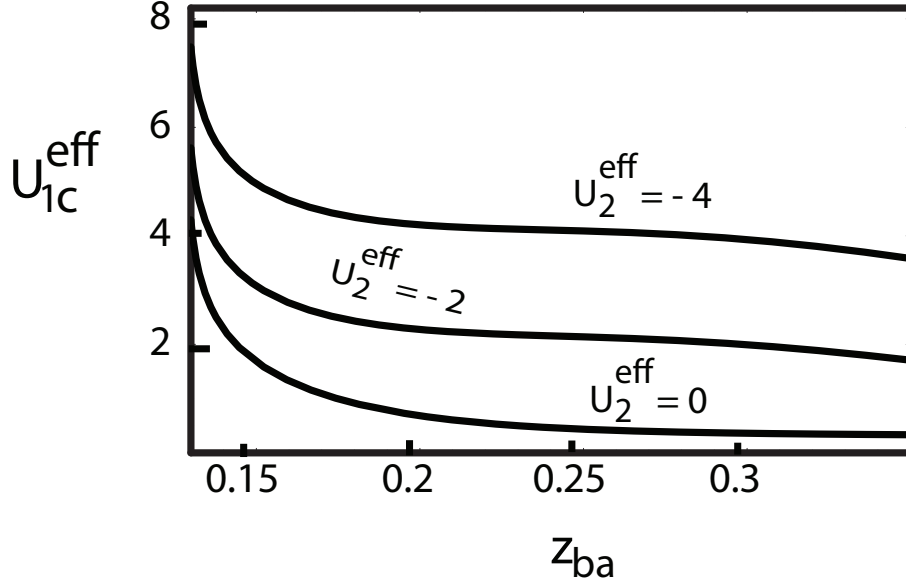


Figure 7: The critical effective potential depth U_{1c}^{eff} versus z_{ba} for parameter values of $|U_2^{eff}| = 4$, $|U_2^{eff}| = 2$, $|U_2^{eff}| = 0$, $z_a = 0.1$ and $z_{we} = 0.16$.

a function of U_2^{eff} for parameter values $z_a = 0.1$, $z_{ba} = z_{we} = 0.16$. When $U_2^{eff} = 0$, $|U_{1c}^{eff}|$, $|U_{3c}^{eff}| = 1.326$ while as $|U_2^{eff}|$ steps up, $|U_{1c}^{eff}|$, $|U_{3c}^{eff}|$ increases revealing the intermediate stickers hindering the lateral phase separation between the short and long stickers. Figure 7 exhibits the plot of $|U_{1c}^{eff}|$, $|U_{3c}^{eff}|$ as a function of z_{ba} for fixed U_1^{eff} , $z_a = 0.1$ and $z_{we} = 0.16$. As z_{ba} increases $|U_{1c}^{eff}|$, $|U_{3c}^{eff}|$ declines; when $|U_2^{eff}|$ steps up $|U_{1c}^{eff}|$, $|U_{3c}^{eff}|$ increases once again shows that the intermediate stickers facilitate mixing of the stickers.

These ideas can easily be checked in experiment by considering vesicle adhesion to supported membrane with several types of stickers. Our theoretical prediction reveals that the presence of intermediate stickers suppresses lateral phase separation. This effect can be checked by incorporating different types of adhesive molecule of different size to membrane surface. As the number of species of stickers increases, lateral phase separation gets suppressed. However lateral phase separation of two or more types of stickers has been observed in experiment. This leads to the conclusion that either nature keeps its types of stickers to a limited number or equilibrium modeling, although it is

simple, fails to capture the phase behavior of membrane with several types of stickers.

5 Summary and conclusion

The equilibrium phase behavior of membranes with stickers of several types is explored at the mean field level. We first consider membranes with short and long stickers. We investigate how the critical potential depth $|U_c^{eff}|$ behaves as the function of the model parameters. The central result shows that $|U_c^{eff}|$ decreases not only as the width and length of the stickers increase but also when z_a increases. In the presence of intermediate stickers, the numerical results uncover that the intermediate stickers hinder the lateral phase separation.

In conclusion, via mean field approximation, we study adhesion induced lateral phase separation of membranes interacting with multiple species stickers of different sizes. Though the mean-field approximation neglects the effect of fluctuations, we believe that the qualitative behavior of the result obtained will not be affected and thus this work is crucial not only for fundamental understanding of the physics of membranes but also for the construction of artificial membranes.

Acknowledgement

I would like to thank Hsuan-Yi Chen for interesting discussions I had during my visit at National Central University, Department of Physics and Graduate Institute of Biophysics, Taiwan. I would like also to thank Thomas Weigl for his helpful comments, suggestions and critical reading of this manuscript. It is my pleasure to thank Chun Biu Li and Prof. Tamiki Komatsuzaki for the interesting discussions and for providing a wonderful research environment.

References

- [1] R. Lipowsky and E. Sackmann., *Structure and Dynamics of Membranes: Generic and Specific Interactions, Vol. 1B of Handbook of Biological Physics* (Elsevier, Amsterdam 1995).
- [2] B. Alberts *et al.*, *Molecular Biology of the Cell*, 3rd edition (Garland, New York, 1994).

- [3] R. Lipowsky, J. Phys. II France **4**, 1755 (1994).
- [4] A. Ammann, R. Lipowsky, J. Phys. II France **6**, 255 (1996).
- [5] Mesfin Asfaw, Physica A **387**, 3526 (2008).
- [6] T. R. Weigl, M. Asfaw, H. Krobath, B. Rozycki and R. Lipowsky, J. Soft matter, DOI: 10.1039/b902017a (2009).
- [7] S. Komura and D. Andelman, Eur. Phys. J. E **3**, 259 (2000).
- [8] R. Bruinsma, A. Behrisch, and E. Sackmann, Phys. Rev. E **61**, 4253 (2000).
- [9] A. Albersdfer, T. Feder, and E. Sackmann, Biophys. J. **73**, 245 (1997).
- [10] T. R. Weigl, R. R. Netz, and R. Lipowsky, Phys. Rev. E **62**, R45 (2000).
- [11] J. Nardi, T. Feder, and E. Sackmann, Europhys. Lett. **37**, 371 (1997).
- [12] T. R. Weigl and R. Lipowsky, Phys. Rev. E **64**, 011903 (2001).
- [13] H. Strey, M. Peterson, and E. Sackmann, Biophys. J. **69**, 478 (1995).
- [14] D. Zuckerman and R. Bruinsma, Phys. Rev. Lett. **74**, 3900 (1995).
- [15] D. Coombs, M. Dembo, C. Wofsy and B. Goldstein, Biophys. J. **86**, 1408 (2004).
- [16] G. I. Bell, M. Dembo and P. Bongrand, Biophys. J. **45**, 1051 (1984).
- [17] M. Dembo and G. I. Bell, Curr. Topics. Memb. Trans. **29**, 71 (1987).
- [18] C. R. F. Monks *et al.*, Nature (London) **395**, 82 (1998); G. Grakoui *et al.*, Science, **285**, 221 (1999); D. M. Davis *et al.*, Proc. Natl. Acad. Sci. U.S.A. **96**, 15062 (1999).
- [19] S. Y. Qi, J. T. Groves, and A. K. Chakraborty, Proc. Natl. Acad. Sci. U.S.A. **98**, 6548 (2001).
- [20] N. J. Burroughs and C. Wlfing, Biophys. J. **83**, 1784 (2002).
- [21] T. R. Weigl and R. Lipowsky, Biophys. J. **87**, 3665 (2004).
- [22] H.-Y. Chen, Phys. Rev. E **67**, 031919 (2003).

- [23] Jia-Yuan Wu and H.-Y. Chen, Phys. Rev. E **73**, 011914 (2006).
- [24] M. Asfaw, B. Rozycki, R. Lipowsky and T. R. Weigl, Europhys. Lett. **76**, 703 (2006).
- [25] Mesfin Asfaw and H.-Y. Chen, Phys. Rev. E. **79**, 041917 (2009).